

PROCEEDINGS OF SPIE

[SPIDigitalLibrary.org/conference-proceedings-of-spie](https://spiedigitallibrary.org/conference-proceedings-of-spie)

First test results from a high-resolution CdZnTe pixel detector with VLSI readout

Walter R. Cook, Steven E. Boggs, Aleksey E. Bolotnikov, Jill A. Burnham, Fiona A. Harrison, et al.

Walter R. Cook, Steven E. Boggs, Aleksey E. Bolotnikov, Jill A. Burnham, Fiona A. Harrison, Branislav Kecman, Brian Matthews, Steven M. Schindler, Michael Fitzsimmons, "First test results from a high-resolution CdZnTe pixel detector with VLSI readout," Proc. SPIE 3769, Penetrating Radiation Systems and Applications, (1 October 1999); doi: 10.1117/12.363688

SPIE.

Event: SPIE's International Symposium on Optical Science, Engineering, and Instrumentation, 1999, Denver, CO, United States

First Test Results from a High Resolution CdZnTe Pixel Detector with VLSI Readout

Walter R. Cook, Steven E. Boggs, Aleksey E. Bolotnikov, Jill A. Burnham, Fiona A. Harrison, Branislav Kecman, Brian Matthews, and Stephen M. Schindler

California Institute of Technology, Pasadena, CA 91125

Michael J. Fitzsimmons

Jet Propulsion Laboratory, Pasadena, CA 91109

ABSTRACT

We are developing a CdZnTe pixel detector with a custom low-noise analog VLSI readout for use in the *High-Energy Focusing Telescope (HEFT)* balloon experiment, as well as for future space astronomy applications. The goal of the program is to achieve good energy resolution (< 1 keV FWHM @ 60 keV) and low threshold in a sensor with ~ 500 μm pixels. We have fabricated several prototype detector assemblies with 2 mm thick, 680 by 650 μm pitch CdZnTe pixel sensors indium bump bonded a VLSI readout chip developed at Caltech. Each readout circuit in the 8 x 8 prototype is matched to the detector pixel size, and contains a preamplifier, shaping amplifiers, and a peak stretcher/discriminator. In the first 8 x 8 prototype, we have demonstrated the low-noise preamplifier by routing the output signals off-chip for shaping and pulse-height analysis. Pulse height spectra obtained using a ^{241}Am source, collimated to illuminate a single pixel, show excellent energy resolution of 1.1 keV FWHM for the 60 keV line at room temperature. Line profiles are approximately Gaussian and dominated by electronic noise, however a small low energy tail is evident for the 60 keV line. We obtained slightly improved resolution of 0.9 keV FWHM at 60 keV by cooling the detector to 5°C , near the expected balloon-flight operating temperature. Pulse height spectra obtained with the collimated source positioned between pixels show the effect of signal sharing for events occurring near the boundary. We are able to model the observed spectra using a Monte-Carlo simulation that includes the effects of photon interaction, charge transport and diffusion, pixel and collimator geometry, and electronic noise. By using the model to simulate the detector response to uncollimated radiation (including the effect of finite trigger threshold for reconstruction of the total energy of multi-pixel events), we find the energy resolution to be degraded by only 10% for full-face illumination, compared to the collimated case. The small value of the degradation is due directly to the low readout noise and amplifier threshold.

Keywords: X-ray astrophysics -- electronics -- CdZnTe

1. INTRODUCTION

With recent advances in the technology of multilayer mirrors, focusing hard X-ray telescopes for astronomical observations are now feasible for energies up to ~ 100 keV. In particular, focusing hard X-ray telescopes are being developed for the balloon-borne payloads *HEFT*¹ and *InFocus*² and for the *Constellation-X* satellite mission. We are developing a CdZnTe pixel detector system for use in the *HEFT* payload and for possible use in *Constellation-X*. The detector consists of a CdZnTe sensor with the anode segmented into pixels indium bump-bonded to a custom VLSI readout chip. The readout supplies a complete pulse-height analysis chain for each pixel. We presented the performance of a four-cell functional prototype of the readout in a previous SPIE paper³. This test chip was not intended for bonding to a detector, but rather had on-chip simulation of the detector capacitance and leakage current. We obtained self-triggering operation over the range 1 - 150 keV with FWHM electronic noise of 50 electrons (approximately 250 eV equivalent energy loss in CdZnTe) for a simulated detector capacitance of 150 fF and negligible leakage current.

In this paper, we present ^{241}Am spectra obtained from a prototype detector assembly consisting of an 8 by 8 cell custom readout chip indium bump-bonded to a CdZnTe pixel detector. We achieved single pixel energy resolution of 1.1 keV FWHM at 60 keV which is, to our knowledge, the best ever measured with a room temperature hard X-ray detector. We discuss the measured spectral results and compare them to Monte Carlo simulations. Using the model, we calculate the effect of multiple pixel events on net energy resolution for flood illumination.

2. DETECTOR and VLSI READOUT

We fabricated several prototype detector assemblies, each consisting of a 7.6 mm x 7.8 mm x 2 mm CdZnTe sensor bonded to an 8 x 8 cell VLSI readout chip. The VLSI chips contain nearly the same circuitry in each pixel cell as the prior 4 cell prototype chip mentioned above. One of the CdZnTe contacts (the anode side) is segmented into an 8 x 8 array with 650 x 680 μm pitch, with each contact measuring 550 by 580 μm , with a 100 μm gap between pixels. Prior study of pixel detector contact geometries indicates that in order to avoid signal loss at the gap between pixels, the inter-pixel gap should be less than about 200 μm ⁴. A guard ring of width 1 mm surrounds the entire pixel array.

The prototype 8 by 8 pixel VLSI chips were manufactured at Orbit Semiconductor using their 1.2 μm CMOS process. Parts were delivered as loose die, with a few in PGA packages. We tested all chips (both with and without CdZnTe detectors attached) mounted in pin grid array (PGA) packages which are easily inserted and removed from a test circuit board supplying power and control signals. We find it very convenient in dealing with these complex chips to avoid any functional testing at a probe station. A typical procedure for a given chip consists of first bonding the chip temporarily into a PGA package using wax for die attach and gold wire ball bonds to the electrical contact pads. We test the packaged chips, and, if good, remove them from the package for indium bump bonding. During chip removal the gold wire bonds are sheered at the ball bond on the chip and the wax dissolved. The wire bond removal causes little damage to the chip's contact pads. Once a CdZnTe detector is attached to a chip, we re-insert the detector assembly into a PGA package, this time using Al bond wire which can be installed at room temperature.

We perform indium bump bonding of the sensor to the readout at JPL's Micro-Devices Laboratory (MDL). Preparation for indium bonding includes the application of a metal layer over the active circuitry of the VLSI chip to serve as an electrostatic shield, preventing unwanted feedback to the pixel contact. We apply a thick (2000 – 3000 Angstrom) aluminum layer using thermal evaporation (e-beam evaporation of a layer of appropriate thickness caused radiation damage to the readout), followed by thin e-beam deposited titanium and platinum layers to act as a barrier against indium diffusion. We have successfully fabricated one chip this way, which functioned normally prior to attachment of the CdZnTe detector. After detector attachment, the chip showed oscillations on all pixels. The detailed structure of the oscillations suggests that the entire electrostatic shield layer is contiguous, but not well grounded. We are in the process of investigating this hypothesis. We are, however, able to study the detector performance by disabling the circuitry downstream of the preamplifier, allowing the output to be routed off-chip via an on-chip precision unity-gain buffer amplifier. We used standard laboratory equipment for further signal amplification, shaping, and pulse height analysis.

For the tests described below, we mounted the test circuit board with detector assembly installed inside a temperature controlled unit below a collimated ^{241}Am source. The source, collimated using a 300 μm diameter hole in a 2 cm thick lead block, can be precisely translated in the transverse dimensions using computer controlled stages. We positioned the source immediately atop the block, while the detector surface (cathode) was positioned approximately 3 mm below the block. This geometry yields a slightly diverging beam of full diameter approximately 390 μm at the detector cathode surface and 450 μm when projected to the anode plane of the 2 mm thick detector. Since the detector pixel dimensions are 680 by 650 μm , we could position the collimated beam in order to illuminate a large portion of a single pixel, without impinging on the neighbors. The axis of the collimator was approximately normal to the detector cathode and anode planes.

3. TEST RESULTS

Figure 1b shows a pulse height spectrum taken with the collimated ^{241}Am source positioned approximately over the center of a pixel. We obtained this spectrum in an over-night run with ambient temperature in the range 23-25 $^{\circ}\text{C}$. We biased the detector at 210 V, producing a pixel leakage current near the maximum (~ 10 pA) that the VLSI preamplifier DC feedback circuit can accommodate. We set the shaping amplifier peak time to approximately 5 μs . The spectrum shows the primary line at 60 keV with a FWHM resolution of 1.1 keV. The numerous lower energy lines from the source as well as the Cd and Te escape lines have Gaussian profiles dominated by the electronic noise, measured with an on-chip test pulser to be 0.83

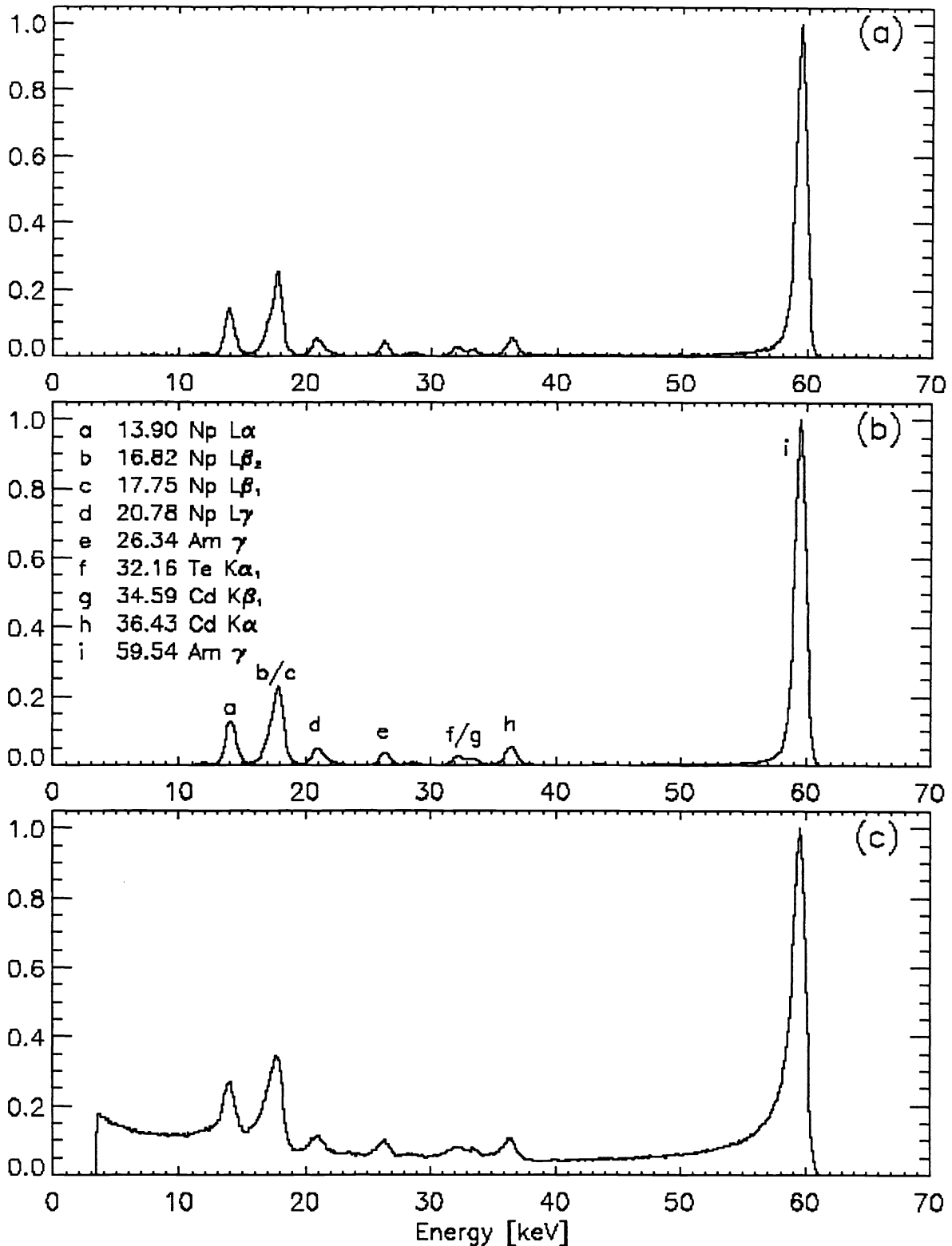


Figure 1: Panel (a) shows the spectrum taken with a ^{241}Am source collimated to the center of a single pixel with the detector operated at 5°C , near the temperature expected in flight. The measured 60 keV energy resolution is 0.9 keV FWHM. Panel (b) shows a room-temperature spectrum, with measured 60 keV resolution of 1.1 keV FWHM. In both cases, the low-energy line resolution is dominated by electronic noise. Panel (c) shows the spectrum taken with the source between pixels, illustrating the effect of charge sharing.

keV FWHM. A slight asymmetry is visible in the 60 keV line profile due to a tail on the low energy side. We obtained a slight improvement in energy resolution by lowering the temperature to near 5 °C, the nominal operating temperature for the balloon-borne telescope. The width of the 60 keV peak dropped to 0.9 keV FWHM due to a reduction in the electronic noise to 0.7 keV FWHM. The spectrum is shown in Figure 1a.

To investigate the effects of charge sharing for events occurring near pixel boundaries, the source beam was positioned directly between two pixels. Pulse height spectra from the two pixels were nearly the same and show broadened line profiles and the continuum as illustrated in Figure 1c.

4. MONTE CARLO SIMULATIONS

Figure 2a compares the Am²⁴¹ spectrum (Figure 1b) to the result of a Monte Carlo simulation. We use a logarithmic vertical scale to allow better viewing of the tail below the 60 keV line. The Monte Carlo model includes the effects of the collimator and pixel geometry, the gamma-ray interactions, the charge transport and diffusion within the CdZnTe, the trapping of holes and electrons within the detector volume, and the measured electronic noise. The simulated spectrum (represented by dots) is close to the actual spectrum, except in the low level continuum near 10 and below 60 keV. Several mechanisms may contribute to the tail below the 60 keV line. The tail seen in the Monte Carlo result is due to 60 keV line photons interacting deep in the detector near the pixel contact. For these events the image charge induced by trapped holes causes a signal reduction. This effect is, however, not sufficient to produce the observed tail. We can exclude the possibility that the discrepancy between the observations and the model arises from events occurring near the pixel boundaries which share some signal with the neighboring pixel (due to diffusion of the electron charge cloud). The beam collimation should have been adequate to prevent such charge sharing, and indeed the spectrum measured after reducing the collimator exit hole diameter from 300 to 200 μm shows the shape and intensity of the tail unchanged.

Figure 2b compares the spectrum obtained with the source positioned between two pixels to the result of a Monte Carlo simulation. The continuum is fairly well matched, and is due to events which interact near enough to the inter-pixel boundary that the electron signal charge cloud, broadened by diffusion to a width near 70 μm, splits across the boundary. We also observed this effect in an earlier pixel detector study⁴. The extent of diffusion depends on the drift time, and therefore on the applied detector bias voltage. We observe that as expected, the level of continuum increases as the bias voltage is reduced.

We also used a Monte Carlo simulation to assess the net energy resolution that would be obtained with full illumination of the detector face, with the signals from shared events summed in post-processing. We assume that individual pixel thresholds are set at 1.5 keV, consistent with the measured electronic noise of 0.7 keV. For events triggering multiple pixels, we summed the energy depositions for all triggered pixels, resulting in an increase in the electronic noise by a factor of the square root of the number of triggered pixels. With the incident photons distributed uniformly over a square region with corners at the center of adjacent pixels, most events (67%) trigger only one pixel, while 30% trigger two pixels, and only 3% trigger more than two. We find the net energy resolution for the 60 keV line to be broadened only slightly to 1.0 keV from the single pixel measured result of 0.9 keV.

5. FUTURE DEVELOPMENT

The immediate goal of our development effort is to verify the expected performance with a fully-functional 8 x 8 pixel prototype detector. We have submitted a new VLSI chip (expected delivery July 19, 1999) with the preamplifier redesigned in order to reduce the electronic noise by better matching the input FET to the actual detector pixel capacitance, which is larger than we originally expected. In addition, the peak stretcher and test pulser have been modified for improved operation. We are investigating processes for producing an effective electrostatic shield layer. In parallel, we have begun layout of the final flight chip, which we expect to submit for fabrication this fall.

6. ACKNOWLEDGEMENTS

This work was supported by the NASA SR&T program under grant No. NAG5-5128.

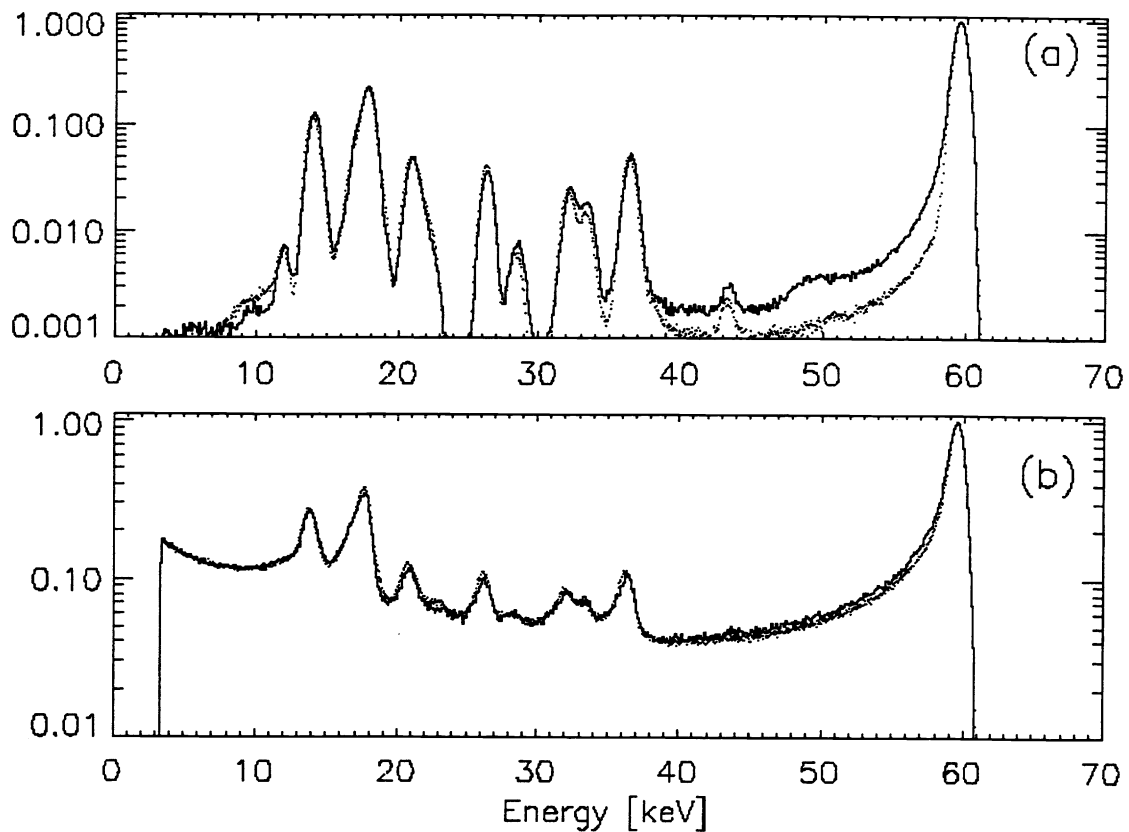


Figure 2: Measured ^{241}Am spectra (solid line) compared to Monte Carlo results (dotted line) plotted on a log intensity scale for ease of comparison. Panel (a) shows results for illumination of the center of a single pixel, and panel (b) shows results for the source positioned in between pixels.

7. REFERENCES

1. P.H. Mao, F.A. Harrison, Y.Y. Platonov, D. Broadway, B. DeGroot, F.E. Christensen, W.W. Craig, and C.J. Hailey, "Development of grazing incidence multilayer mirrors for hard X-ray focusing telescopes", *Proc. of SPIE* 3114, 1997
2. K. Tamura, K. Yamashita, H. Kunieda, Y. Tawara, A. Furuzawa, K. Haga, G.S. Lodha, N. Nakajo, N. Nakamura, Takashi Okajima, Osamu Tsuda, P.J. Serlemitsos, J. Tueller, R. Petre, Y. Ogasaka, Y. Soong, and K. Chan, "Development of balloon-borne hard X-ray telescopes using multilayer supermirror", *Proc. of SPIE* 3113, pp. 285 – 292, 1997.
3. W.R. Cook, Jill A. Burnham, and Fiona A. Harrison, "Low-noise custom VLSI fo CdZnTe pixel detectors", *Proc. of SPIE* 3445, pp. 347-354, 1998
4. A.E. Bolotnikov, W.R. Cook, F.A. Harrison, A.-S. Wong, S.M. Schindler, and E.C. Eichelberger, "Charge loss between contacts of CdZnTe pixel detectors", accepted for publication in *Nuclear Instruments and Methods*